Journal of Experimental Botany, Vol. 61, No. 11, pp. 3015–3028, 2010
doi:10.1093/jxb/erq128 Advance Access publication 19 May, 2010
This paper is available online free of all access charges (see http://jxb.oxfordjournals.org/open_access.html for further details)

Journal of Experimental Botany
www.jxb.oxfordjournals.org

RESEARCH PAPER

Photosynthesis at an extreme end of the leaf trait spectrum: how does it relate to high leaf dry mass per area and associated structural parameters?

Foteini Hassiotou[1,3,*], Michael Renton[1,2], Martha Ludwig[3], John R. Evans[4] and Erik J. Veneklaas[1]

[1] School of Plant Biology, Faculty of Natural and Agricultural Sciences, The University of Western Australia, 35 Stirling Highway, Crawley WA 6009, Australia

[2] CSIRO Sustainable Ecosystems, Floreat, WA 6014, Australia

[3] School of Biomedical, Biomolecular and Chemical Sciences, Faculty of Life and Physical Sciences, The University of Western Australia, 35 Stirling Highway, Crawley WA 6009, Australia

[4] Plant Science Division, Research School of Biology, Australian National University, Canberra, ACT 2601, Australia

* To whom correspondence should be addressed. E-mail: foteini.hassiotou@uwa.edu.au

Received 19 February 2010; Revised 12 April 2010; Accepted 19 April 2010

Abstract

Leaf dry mass per area (*LMA*) is a composite parameter relating to a suite of structural traits that have the potential to influence photosynthesis. However, the extent to which each of these traits contributes to variation in *LMA* and photosynthetic rates is not well understood, especially at the high end of the *LMA* spectrum. In this study, the genus *Banksia* (Proteaceae) was chosen as a model group, and key structural traits such as *LMA*, leaf thickness, and density were measured in 49 species. Based on the leaf trait variation obtained, a subset of 18 species displaying a wide range in *LMA* of 134–507 g m^{-2} was selected for analyses of relationships between leaf structural and photosynthetic characteristics. High *LMA* was associated with more structural tissue, lower mass-based chlorophyll and nitrogen concentrations, and therefore lower mass-based photosynthesis. In contrast, area-based photosynthesis did not correlate with *LMA*, despite mesophyll volume per area increasing with increases in *LMA*. Photosynthetic rate per unit mesophyll volume declined with increasing *LMA*, which is possibly associated with structural limitations and, to a lesser extent, with lower nitrogen allocation. Mesophyll cell wall thickness significantly increased with *LMA*, which would contribute to lower mesophyll conductance at high *LMA*. Photosynthetic nitrogen use efficiency and the nitrogen allocation to Rubisco and thylakoids tended to decrease at high *LMA*. The interplay between anatomy and physiology renders area-based photosynthesis independent of *LMA* in *Banksia* species.

Key words: Gas exchange, leaf density, LMA, leaf internal conductance, leaf thickness, mesophyll conductance, photosynthesis, sclerophylly.

Introduction

In multispecies analyses, the area-based photosynthetic rate correlates poorly with dry mass per unit leaf area (*LMA*), whereas mass-based photosynthesis shows a clear decline with increasing *LMA* (Reich *et al.*, 1997; Wright *et al.*, 2004). While the second observation may be explained by the greater proportion of structural (non-photosynthetically

Abbreviations: A_{area}, net CO_2 assimilation rate per unit leaf area; A_{Chl}, net CO_2 assimilation rate per unit chlorophyll; A_{mass}, net CO_2 assimilation rate per unit leaf mass; A_{mes}, net CO_2 assimilation rate per unit mesophyll; $Chl_{mesophyll}$, chlorophyll concentration per mesophyll volume; D_{leaf}, leaf density; D_{leaf}^*, leaf density corrected for porosity; f_{crypt}, the fraction of the leaf cross-section occupied by crypts; $f_{epidermis}$, the fraction of the leaf cross-section occupied by epidermis and hypodermis; f_{air}, the fraction of the leaf cross-section occupied by airspaces; $f_{mesophyll}$, the fraction of the leaf cross-section occupied by mesophyll; $f_{vascular}$, the fraction of the leaf cross-section occupied by vascular tissue; g_{leaf}, leaf conductance to CO_2; g_m, mesophyll conductance to CO_2; *LMA*, leaf dry mass per unit leaf area; L_P, adaxial palisade cell length; *LVA*, leaf volume per unit leaf area; *MVA*, mesophyll volume per unit leaf area; N_{area}, nitrogen per unit leaf area; N_{mass}, nitrogen per unit leaf mass; *PNUE*, photosynthetic nitrogen use efficiency; $T_{epidermis,B}$, thickness of abaxial epidermis and hypodermis; $T_{epidermis,T}$, thickness of adaxial epidermis and hypodermis; T_{leaf}, leaf lamina thickness; $T_{mesophyll}$, mesophyll thickness; T_w, mesophyll cell wall thickness.

active) tissue per unit leaf dry mass, which is also expressed as lower mass-based nutrient concentrations (Chapin, 1980), it is less clear how high-*LMA* leaves are able to fix CO_2 at rates that are similar to those of low-*LMA* leaves that are usually found on fast-growing plants.

LMA is a key structural trait that measures the investment of dry mass per unit of light-intercepting leaf area and is widely used as an indicator of plant ecological strategies (Westoby *et al.*, 2002; Wright *et al.*, 2004). High *LMA* can be due to a thick leaf or high leaf density, or both (Witkowski and Lamont, 1991). High-*LMA* leaves are often hard, and referred to as sclerophylls (Turner, 1994), although succulent species can also display high *LMA* values due to high leaf thickness (Poorter *et al.*, 2009). In the present study, *LMA* and its relationship with photosynthesis is discussed in the context of hard, thick, and dense leaves of a wide range of *LMA*, with robust construction, which confers long lifespans.

Despite the general anatomical organization of high-*LMA* leaves, which are thick and/or dense, fibrous, and often hairy, at least on the abaxial surface (Turner, 1994; Read *et al.*, 2000; Mast and Givnish, 2002), the structural traits at the tissue and cell level that contribute to high *LMA* are particularly diverse and include bundle fibre caps, lignified bundle sheaths, vascular bundle extensions, lignified leaf margins, very thick cuticles, lignified hypodermal structures associated with the adaxial and/or abaxial surfaces, sclereids within the mesophyll, sclereids associated with vein endings, and thick cell walls (Dillon, 2002; Terashima *et al.*, 2006). It must be noted that some of these characters are not restricted to high-*LMA* leaves, and not all high-*LMA* species possess all of these characters (Read *et al.*, 2000). In other words, different combinations of the above leaf traits can result in high *LMA* (Read *et al.*, 2000; Read and Sanson, 2003), and this explains the great variation in this trait that is usually found among hard leaves (Read *et al.*, 2000), even within the same genus (Hassiotou *et al.*, 2009*a*). While it is clear that variation in leaf thickness and density is due to the number of cell layers (photosynthetic or not) and the relative amount of cell types, respectively, the relative importance of these structural traits in determining thickness, density, and *LMA* is not well understood.

High *LMA* has been associated with low conductance to CO_2 diffusion from the substomatal cavity to the chloroplasts (mesophyll conductance, g_m), which can restrict the rate of CO_2 assimilation (Loreto *et al.*, 1992; Evans *et al.*, 1994; Parkhurst, 1994; Evans and von Caemmerer, 1996; Evans and Loreto, 2000; Terashima *et al.*, 2006; Hassiotou *et al.*, 2009*a*). Moreover, surface properties of high-*LMA* leaves, including wax layers, epidermal cell shape, cuticular thickening, trichomes, and stomatal crypts, as well as specific scleromorphic structures, such as sclereids, can alter leaf optical properties (Myers *et al.*, 1994; Baldini *et al.*, 1997) and thus influence gas exchange. High-*LMA* leaves have low concentrations of key nutrients such as nitrogen, but whether this is simply due to 'dilution' by the presence of more structural tissue, or also applies to the photosynthetically active mesophyll, is not known. In fact, it is unclear whether the photosynthetically active mesophyll cells of high-*LMA* leaves differ from those in lower *LMA* leaves and, if so, whether this is because of the conditions in which they operate (CO_2, light) or because they are structurally and/or physiologically different.

To advance our understanding of the physiological consequences of leaf structure, the genus *Banksia* L.f. (Proteaceae), being predominantly endemic to Australia, was used as a model group on the basis of the great leaf structural diversity that it displays (*LMA*=134–507 g m^{-2}; Hassiotou *et al.*, 2009*a*). Key leaf structural traits such as *LMA*, leaf thickness, and density were examined in 49 *Banksia* species. Subsets of this large group representative of the diversity found in this genus were subsequently selected to investigate inter-relationships between leaf structure and photosynthesis. The following questions were asked:

(i) How much of the variability in *LMA* is due to variability in leaf thickness and how much to variability in leaf density in *Banksia*, and which anatomical parameters correlate most strongly with leaf thickness and density?

(ii) How does the light-saturated rate of photosynthesis at ambient CO_2 relate to leaf structural parameters at the high end of the *LMA* spectrum? If, as in previous studies, area-based photosynthetic rate does not correlate with *LMA*, is that because high-*LMA* leaves do not pack more photosynthetic tissue per unit leaf volume, or because this tissue is less efficient than that in low-*LMA* leaves?

(iii) How do chlorophyll and nitrogen content and the components of photosynthetic nitrogen use efficiency (*PNUE*) vary with *LMA*?

Materials and methods

Plant material and growth conditions

Three- to 5-year old plants of 49 broad-leaved (as opposed to needle-leaved) *Banksia* species were used (see Appendix). The plants, except for *B. integrifolia* L.f., *B. paludosa* R.Br., and *B. serrata* L.f., were grown from seed in 10.0 l pots containing a mixture of river sand and potting mix, in Perth (Australia), outdoors (with an average annual temperature and average daily solar exposure of 19 °C and 20 MJ m^{-2}, respectively; Australian Government, Bureau of Meteorology) until ~3 weeks before the measurements, when they were transferred to a controlled-temperature greenhouse (23 °C day/18 °C night). Mature plants of *B. integrifolia*, *B. paludosa*, and *B. serrata* were purchased from a nursery in Canberra (Australia). Upon purchase, the plants were re-potted into 10.0 l pots containing a mixture of grey sand and potting mix, and grown for 2 months prior to measurements in a greenhouse in Canberra (25 °C day/20 °C night). Key leaf traits, such as *LMA*, leaf thickness, and density, were measured in all 49 species. With the aim of always covering the wide range of *LMA* observed in the genus *Banksia*, subsets of this large group representative of the diversity observed across the genus were selected for further structural and physiological analyses. In all cases, the youngest fully expanded leaves were used. For a list of the traits obtained for each species see the Appendix.

Leaf morphology and anatomy

Three leaves per species, from different plants, were sampled early in the morning. Leaf lamina thickness (T_{leaf}) was measured with digital callipers at 5–10 different positions on each leaf. The midrib and petiole were removed prior to measuring the projected area of the lamina using a leaf area meter (LI-300A, Li-Cor, Lincoln, NE, USA). After drying at 80 °C for 3 d, leaf lamina dry mass was measured. Leaf dry tissue density (D_{leaf}) was computed from LMA and T_{leaf}:

$$D_{leaf} = LMA/T_{leaf} \quad (1)$$

Based on the relationship between LMA and T_{leaf} and D_{leaf}, subsets of species that covered the range of LMA of the 49 species were chosen for further analyses (Appendix).

In three leaves per species, for 14 species (Appendix), the fraction of the leaf volume filled with air (f_{air}) was measured by determining leaf buoyancy before and after vacuum infiltration of the leaf air spaces with water, using the method of Raskin (1983) and the equations modified by Thomson *et al.* (1990). In brief, fresh leaf volume (V_{leaf}), leaf gas volume (V_{gas}), and f_{air} were estimated as:

$$V_{leaf} = \frac{M_{leaf,\,in\,air} - M_{leaf,\,in\,water}}{\rho} \quad (2)$$

$$V_{gas} = \frac{M_{leaf,\,after} - M_{leaf,\,before}}{\rho} \quad (3)$$

$$f_{air} = \frac{V_{gas}}{V_{leaf}} \quad (4)$$

where $M_{leaf,\,in\,air}$ and $M_{leaf,\,in\,water}$ are the masses of the leaf in air and water before vacuum infiltration, respectively; $M_{leaf,\,after}$ and $M_{leaf,\,before}$ are the masses of the submerged leaf holder with the leaf after and before vacuum infiltration, respectively; and ρ is the density of water (1 mg mm^{-3} at 25 °C).

The density of the fresh leaf tissues excluding the gas volumes (leaf density corrected for porosity, D_{leaf}*) was calculated as:

$$D_{leaf}* = \frac{M_{leaf}}{(V_{leaf} - V_{gas})} \quad (5)$$

where M_{leaf} is leaf dry mass.

Chemical composition

Nitrogen concentration (N_{mass}) was measured in the leaf blade (excluding the midrib) in 17 species (Appendix) using gas chromatography (Carlo Erba EA 1110). Analyses of 14 species were done at the Western Australian Biogeochemistry Centre (University of Western Australia, Perth). Samples from the other three species (*B. integrifolia*, *B. paludosa*, and *B. serrata*) were analysed at the Research School of Biology (Australian National University, Canberra). Finely ground leaf dry matter was used from three leaves per species from three different plants, except for *B. attenuata* and *B. ilicifolia* where one leaf was analysed. N_{area} was subsequently calculated (N_{area}=N_{mass}×LMA).

The fraction of nitrogen allocated to Rubisco (R_N/N) was estimated (Appendix) as:

$$\frac{R_N}{N} = \frac{V_c \times \frac{M_R}{k_{cat}} \times \frac{N_R}{n_R}}{N_{area}} \quad (6)$$

where V_c is the rate of carboxylation, computed using the spreadsheet published by Sharkey *et al.* (2007), but using chloroplastic CO_2 concentration (C_c) calculated by combined gas exchange and chlorophyll fluorescence (Hassiotou *et al.*, 2009*a*); M_R is the molecular mass of Rubisco [0.55 g of Rubisco (μmol Rubisco)$^{-1}$]; k_{cat} is the catalytic turnover number at 25 °C [3.5 mol CO_2 (mol Rubisco sites)$^{-1}$ s^{-1}; von Caemmerer *et al.*, 1994]; n_R is the number of catalytic sites per mole of Rubisco [8 mol Rubisco sites (mol Rubisco)$^{-1}$]; N_R is the nitrogen concentration of Rubisco [11.4 mmol N (g Rubisco)$^{-1}$]; and N_{area} is the nitrogen content per unit leaf area (mmol N m^{-2}). It was assumed that k_{cat} did not vary between *Banksia* species or with LMA, but the absolute fraction of nitrogen present in Rubisco could differ if k_{cat} or the activation state varied between the species. Equation 6 provides a minimum estimate of R_N/N as it assumes full Rubisco activation (Harrison *et al.*, 2009).

Total chlorophyll content (Chl_{area}) was determined in 12 species (Appendix) using three leaves per species from three different plants, sampled early in the morning and analysed immediately. Leaf segments were excised and their areas were measured with a leaf area meter (LI-300A, Li-Cor, Lincoln, NE, USA). Within 5 min of sampling, the leaf segments were finely ground with liquid nitrogen using a cold mortar and pestle and were subsequently extracted with 100% cold methanol. The extract was clarified by centrifugation at 1600 *g* (Beckman, Avanti™ J-25 Centrifuge, USA) for 20 min at 4 °C. To avoid condensation on the cuvette whilst taking measurements, the samples were stored in the dark at room temperature for 5 min. Absorbance was measured with a spectrophotometer (Graphicord UV-240, Shimadzu, Kyoto, Japan) at three wavelengths (710, 665.2, and 652.4 nm) and the equations of Wellburn (1994) were used to calculate *Chla*, *Chlb*, total chlorophyll per unit leaf area (Chl_{area}), and dry mass (Chl_{mass}). The fraction of nitrogen allocated to thylakoids (T_N/N), including pigment–protein complexes, the components of electron transport, and ATPase, was estimated from Chl_{area} and N_{area}, assuming 50 mol of thylakoid nitrogen per mol of chlorophyll (Evans, 1989).

Microscopy

Cryo-scanning electron microscopy (CSEM) and fluorescence microscopy (Zeiss Axioskop2, Zeiss Axiocam with AxioVision software, Zeiss Oberkocken, Germany) were used to obtain transverse views of leaf laminas originating halfway from the leaf tip in samples from two leaves per species, from different plants. Analyses were done in Image J (Abramoff *et al.*, 2004). Figure 1 shows diagrammatically how the anatomical measurements were made. Leaf thickness (T_{leaf}), mesophyll thickness ($T_{mesophyll}$), and the thickness of the adaxial ($T_{epidermis,T}$) and abaxial ($T_{epidermis,B}$) epidermis plus hypodermis ($T_{epidermis,B}$) were measured from fluorescence micrographs taken at the same magnification in a subset of 10 species (Appendix), and the mean of at least six measurements was used. These measurements were confirmed with CSEM.

Leaf lamina thickness and mesophyll thickness do not take into account the presence of stomatal crypts. Thus, micrographs of transverse leaf views obtained with fluorescence microscopy at the same magnification, were used to calculate leaf volume per area (LVA) and mesophyll volume per area (MVA) which exclude the volumes taken by crypt voids. The width of an areole (W_{areole}) and the cross-sectional area of non-photosynthetic tissue per areole (A_1) (including the adaxial and abaxial epidermal and hypodermal tissues as well as the vascular bundles and their sclerified extensions) and of mesophyll tissue per areole (A_2) (including photosynthetic cells and intercellular airspaces) were measured. A mean of at least four measurements for each of the above parameters was obtained. LVA and MVA were calculated as:

$$LVA = \frac{A_1 + A_2}{W_{areole}} \quad (7a)$$

$$MVA = \frac{A_2}{W_{areole}} \quad (7b)$$

The leaf tissue was analysed by considering five compartments: the epidermis/hypodermis, mesophyll, intercellular airspace, vascular tissue, and stomatal crypts. The fraction of the leaf

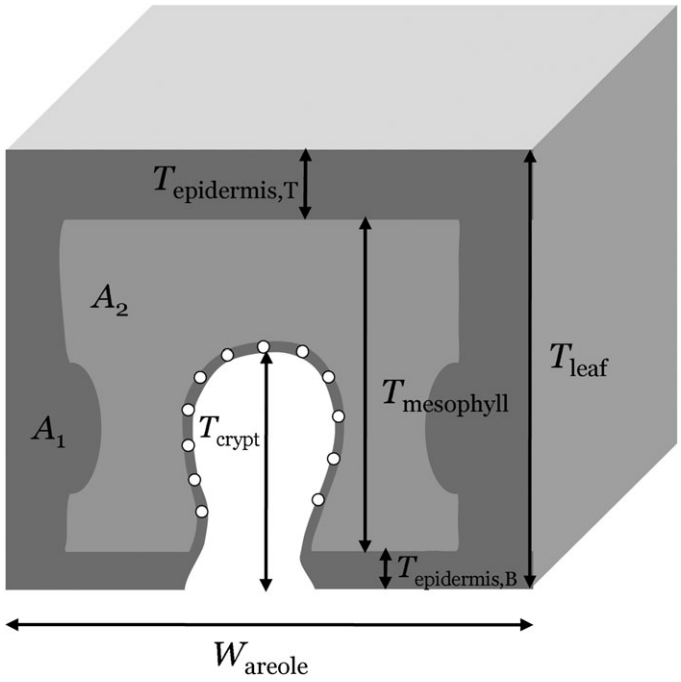

Fig. 1. Diagrammatic representation of a single areole showing the leaf anatomical measurements made. Leaf lamina thickness (T_{leaf}) was measured microscopically as the vertical distance between the adaxial and abaxial cuticle. Mesophyll thickness ($T_{mesophyll}$) was measured as the distance between the adaxial and abaxial epidermis, between the crypt and the vein (i.e. at its maximum). The thicknesses of the adaxial ($T_{epidermis,T}$) and abaxial ($T_{epidermis,B}$) combined epidermis and hypodermis as well as the thickness (depth) of the crypt were measured at the points shown. Two cross-sectional areas were measured: A_1 (shown in dark grey), which represents the non-photosynthetic tissue of an areole, including the adaxial and abaxial epidermal and hypodermal tissues as well as the vascular bundles and their sclerified extensions; and A_2 (shown in light grey), which represents the mesophyll tissue of an areole, including photosynthetic cells and intercellular airspaces. The width of an areole (W_{areole}) was also measured as shown. From the above, leaf volume per area (*LVA*) and mesophyll volume per area (*MVA*) were calculated (Equations 7a and b, respectively).

cross-section occupied by epidermis ($f_{epidermis}$) was calculated as the sum of the fractions associated with the adaxial and abaxial epidermis including hypodermal layers. The adaxial epidermis fraction ($f_{epidermis,T}$) was:

$$f_{epidermis,T} = \frac{T_{epidermis,T}}{T_{leaf}} \quad (8a)$$

The abaxial epidermis fraction ($f_{epidermis,B}$) was:

$$f_{epidermis,B} = \frac{T_{epidermis,B}}{T_{leaf}}\left(1 - A_{crypt} \times D_{crypt}\right) \quad (8b)$$

where the second part of this formula accounts for the portion of the abaxial epidermis and hypodermis that is occupied by crypts, with A_{crypt} the projected area of an average crypt and D_{crypt} the number of crypts per unit projected area. A_{crypt} and D_{crypt} were measured in scanning electron micrographs of the adaxial leaf surface as described in Hassiotou *et al.* (2009*b*). The fraction of the leaf cross-section occupied by mesophyll ($f_{mesophyll}$) was calculated as:

$$f_{mesophyll} = \frac{A_2}{A_1 + A_2} = \frac{MVA}{LVA} \quad (8c)$$

The fraction of the leaf cross-section occupied by vascular tissue (including vascular bundle extensions), $f_{vascular}$, was obtained from $f_{epidermis}$ and $f_{mesophyll}$ based on the assumption that:

$$f_{epidermis} + f_{mesophyll} + f_{vascular} = 1 \quad (8d)$$

Although the crypts are external to the leaf and thus do not contribute to *LVA*, for ease of comparison, crypt volume is expressed as a fraction of the leaf volume:

$$f_{crypt} = \frac{A_{crypt} \times D_{crypt} \times T_{crypt}}{LVA} \quad (8e)$$

where T_{crypt} is the depth of the crypt, using values from Hassiotou *et al.* (2009*b*).

Usually one layer, but sometimes locally two layers, of adaxial palisade mesophyll is present in *Banksia* leaves. The length of adaxial palisade cells ($L_{palisade}$) was measured as the mean of at least seven measurements in transverse views of five species (Appendix) obtained with CSEM at the same magnification.

Wall thickness of palisade and spongy mesophyll cells was measured in six species (Appendix) and mean mesophyll cell wall thickness was calculated (T_w). Leaves of these species were frozen in liquid nitrogen and high-magnification images of the cell walls were obtained with CSEM following McCully *et al.* (2004). Segments of the leaf lamina from the middle part of each leaf were excised under liquid nitrogen, mounted on stubs with low-temperature Tissue-Tek (OCT Compound cryostat specimen matrix, ProSciTech), planed flat in the paradermal and transverse direction using a diamond knife in a cryomicrotome (Cryo-system Oxford CT1500, Oxford Instruments Ltd, Eynsham, Oxford, UK) at –100 °C, etched in the column of the CSEM (Cambridge S360, Cambridge Instruments Ltd, Cambridge, UK) for 1–2 min at –90 °C to reveal cell outlines, sputter-coated with gold, and examined at 15 kV. Images were captured using Microsoft Photodraw and analysed in Image J (Abramoff *et al.*, 2004).

Photosynthetic measurements

Gas exchange measurements were carried out for 18 species (Appendix) using three leaves per species from different plants, at a photosynthetic photon flux density of 1500 μmol quanta m^{-2} s^{-1}, at 380 μmol CO_2 mol^{-1} air, and at 25 °C, with a LI-6400 open gas exchange system (LI-6400-40, Li-Cor, Lincoln, NE, USA). Leaves were kept in the gas exchange chamber at high irradiance (1500 μmol quanta m^{-2} s^{-1}) and low CO_2 concentration (100 μmol CO_2 mol^{-1} air) for at least 10 min before the commencement of the measurements, ensuring stomata were fully open and steady state was reached. At ambient CO_2 concentration, 4–10 measurements of gas exchange, at least 7 s apart, were recorded for each leaf, and the mean value of the net CO_2 assimilation rate was calculated and expressed on a leaf area basis (A_{area}, μmol m^{-2} s^{-1}), on a leaf mass basis (A_{mass}=A_{area}/*LMA*, nmol g^{-1} s^{-1}), per unit *Chl* (A_{Chl}=A_{area}/*Chl*, μmol g^{-1} s^{-1}), per unit mesophyll volume (A_{mes}=A_{area}/*MVA*, μmol m^{-3} s^{-1}), and per unit nitrogen (*PNUE*=A_{mass}/N_{mass}, nmol g^{-1} s^{-1}).

Combined gas exchange and chlorophyll fluorescence measurements (Harley *et al.*, 1992) were conducted and mesophyll conductance (g_m) was calculated in seven species (Appendix) as described in Hassiotou *et al.* (2009*a*).

Statistical analyses

Following previous studies (e.g. Poorter *et al.*, 2009), the aim was to identify the extent to which T_{leaf} and D_{leaf}, the two determinants

of the key structural trait *LMA*, contributed to its variation across the 49 *Banksia* species (see Appendix).

Log–log scaling slope analysis is a method that has been used previously (e.g. Poorter and van der Werf, 1998; Poorter *et al.*, 2009) to estimate the contribution of explanatory variables (such as T_{leaf} and D_{leaf}) to variation in a particular variable of interest (such as *LMA*). This method is based on the relationship $LMA=T_{leaf}\times D_{leaf}$ and thus $\log(LMA)=\log(T_{leaf})+\log(D_{leaf})$, which is exact in this case due to the fact that D_{leaf} was calculated from measured *LMA* and T_{leaf}. If the log of an explanatory variable (in this case either T_{leaf} or D_{leaf}) is fitted as a linear model of the log of the variable of interest (in this case *LMA*), then a slope coefficient value of close to 1 is supposed to indicate that the particular explanatory variable used is largely responsible for variation in the variable of interest, whereas a value close to 0 indicates that the particular explanatory variable used is not responsible for much of the observed variation in the variable of interest (Poorter and van der Werf, 1998; Poorter *et al.*, 2009). However, this method has potential problems when explanatory variables are positively or negatively correlated. This method was thus applied in the present study to enable comparison with previous literature, but the contribution of T_{leaf} and D_{leaf} to variation in *LMA* was also evaluated using a simple and more transparent alternative method.

This simple alternative method is based on the fact that $\log(LMA)=\log(T_{leaf})+\log(D_{leaf})$, and thus $\mathrm{var}[\log(LMA)]=\mathrm{var}[\log(T_{leaf})]+\mathrm{var}[\log(D_{leaf})]+2\times\mathrm{cov}[\log(T_{leaf}),\log(D_{leaf})]$. If the contributing variables $\log(T_{leaf})$ and $\log(D_{leaf})$ are not correlated then the covariance component $2\times\mathrm{cov}[\log(T_{leaf}),\log(D_{leaf})]$ will be relatively small and thus contribute little to the observed variability in $\log(LMA)$. If the contributing variables $\log(T_{leaf})$ and $\log(D_{leaf})$ are (positively or negatively) correlated then the covariance component will be relatively large (and positive or negative, respectively), and thus contribute substantially to the observed variability in $\log(LMA)$. The respective contributions of the three components $\mathrm{var}[\log(T_{leaf})]$, $\mathrm{var}[\log(D_{leaf})]$, and $2\times\mathrm{cov}[\log(T_{leaf}),\log(D_{leaf})]$ to $\mathrm{var}[\log(LMA)]$ were thus simply calculated. Note that these three contributions must sum to 100%. If the contribution of $2\times\mathrm{cov}[\log(T_{leaf}),\log(D_{leaf})]$ is small, then the variables are relatively uncorrelated, and it makes sense to compare the other two contributions to determine whether variability in *LMA* is due more to variability in T_{leaf} or D_{leaf}, or whether they are contributing similarly. If the contribution of $2\times\mathrm{cov}[\log(T_{leaf}),\log(D_{leaf})]$ is large (positive or negative), then the variables are relatively correlated, and the interpretation must be much more cautious. The correlation coefficient between $\log(T_{leaf})$ and $\log(D_{leaf})$ was also calculated, for reference as a more commonly used measure of correlation. Note that in most cases, the results of the two methods would be expected to support each other, but in particular cases discrepancies between these methods could highlight issues that need further investigation (such as high correlation between explanatory variables). Note that both these approaches are not investigating which of T_{leaf} and D_{leaf} contributes most to *LMA*, but rather which contributes most to variation in *LMA*.

These two approaches were also used to examine the main determinants of the variation in D_{leaf} (D_{leaf}* and f_{air}) in 14 species (Appendix), using the equation:

$$D_{leaf} = \left(1 - f_{air}\right)\times D_{leaf^*} \quad (9)$$

and using log transformations to make the relationship additive. This again describes an exact relationship, because of how D_{leaf}* was calculated. The two approaches were again used to examine the main determinants of the variation in T_{leaf} ($T_{mesophyll}$, $T_{epidermis,B}$, and $T_{epidermis,T}$) in 10 species (Appendix), but since the relationship between T_{leaf} and its components is additive rather than multiplicative ($T_{leaf}=T_{mesophyll}+T_{epidermis,B}+T_{epidermis,T}$), the methods were applied directly to the original values of the different thicknesses, without log transformation. Also, in this case the relationship was not exact as all thicknesses were measured independently. As there were three contributing variables involved, four contributions to variance were calculated, the three contributions due to variability in $T_{mesophyll}$, $T_{epidermis,B}$ and $T_{epidermis,T}$, and the covariance contribution, which is equal to $2[\mathrm{cov}(T_{mesophyll}, T_{epidermis,B})+\mathrm{cov}(T_{mesophyll}, T_{epidermis,T})+\mathrm{cov}(T_{epidermis,T}, T_{epidermis,B})]$. The three correlation coefficients between $T_{mesophyll}$, $T_{epidermis,B}$, and $T_{epidermis,T}$ were also calculated to complete the picture.

To help understand the variability in A_{area}, two relationships were considered. The first relationship aimed at assessing if variation in A_{area} was due mostly to differences in the amount of mesophyll tissue or in the mesophyll's photosynthetic activity:

$$A_{area} = f_{mesophyll}\times A_{mes}\times LVA \quad (10)$$

where $f_{mesophyll}$ is the mesophyll volume faction ($m^3\ m^{-3}$), A_{mes} is the CO_2 assimilation rate per mesophyll ($\mu mol\ m^{-3}\ s^{-1}$), and *LVA* is leaf volume per area ($m^3\ m^{-2}$). The second relationship considered for A_{area} aimed at assessing if variation in A_{area} was related more to differences in the amount of chlorophyll or in the photosynthetic rate per unit chlorophyll:

$$A_{area} = Chl_{mes}\times A_{Chl}\times MVA \quad (11)$$

where Chl_{mes} is the chlorophyll concentration per mesophyll volume ($g\ m^{-3}$), A_{Chl} is CO_2 assimilation rate per chlorophyll ($\mu mol\ g^{-1}\ s^{-1}$), and *MVA* is the mesophyll volume per unit leaf area ($m^3\ m^{-2}$). These two relationships were converted from multiplicative to additive relationships by taking the log of the various variables. Both these relationships were exact, due to the fact that one of the variables in each of the equations had been calculated from the others, and both involved three contributing variables. All these above analyses were conducted using the R statistical program (R Development Core Team 2009).

To examine whether $T_{epidermis,T}$ was significantly different from $T_{epidermis,B}$, a paired *t*-test was carried out (Microsoft Excel® 2007, Microsoft Corporation).

Results

LMA and its anatomical correlates

Among the 49 broad-leaved *Banksia* species examined, *LMA* varied 4-fold (134–507 $g\ m^{-2}$), which was associated with a 4-fold variation in leaf lamina thickness (T_{leaf}; 193–700 μm) and a 3-fold variation in leaf density (D_{leaf}; 0.41–1.17 $mg\ mm^{-3}$). Both T_{leaf} and D_{leaf} were approximately equally good predictors of *LMA*, as indicated by both the variance partitioning and the log–log scaling slope analyses (Table 1). Some species had high *LMA* due to their high D_{leaf} and others due to their high T_{leaf}, whilst in some high *LMA* was due to both (Fig. 2). For example, both *B. coccinea* and *B. quercifolia* had an *LMA* of 215 $g\ m^{-2}$, but a T_{leaf} of 0.50 mm and 0.38 mm, and a D_{leaf} of 0.4 $mg\ mm^{-3}$ and 0.6 $mg\ mm^{-3}$, respectively.

Thicker leaves, with high volume per area (*LVA*), had thicker mesophyll ($T_{mesophyll}$), adaxial ($T_{epidermis,T}$), and abaxial ($T_{epidermis,B}$) epidermis and hypodermis, greater mesophyll volume per area (*MVA*), and longer adaxial palisade cells ($L_{palisade}$) (Fig. 3, Table 1). Both statistical analyses used to examine the contributions of the variability in the thickness of the different leaf layers to the variability in T_{leaf} indicated that the $T_{mesophyll}$ contributed most to the variability of T_{leaf}, although variability in $T_{epidermis,T}$ and $T_{epidermis,B}$ also contributed to variability in T_{leaf} (Table 1).

Table 1. Results of analyses of the relative contribution of explanatory variables to measured structural and physiological variables: variance partitioning between contributing factors and covariance, correlation between contributing factors (*r*), and log–log scaling slope analysis (slope)

	n	% due to variance	% due to covariance	*r*	Slope
†D_{leaf} to *LMA*	49	63%	–38%	–0.27	0.43***
T_{leaf} to *LMA*	49	75%			0.57***
†D_{leaf}* to D_{leaf}	14	61%	30%	0.63	0.76***
(*1–*f_{air}) to D_{leaf}	14	9%			0.24**
$T_{mesophyll}$ to T_{leaf}	10	60%	27%	0.59, 0.26, 0.30	0.74***
$T_{epidermis,B}$ to T_{leaf}	10	0.3%			0.04*
$T_{epidermis,T}$ to T_{leaf}	10	12%			0.16 ns
†A_{mes} to A_{area}	10	424%	–697%	–0.76, –0.19, –0.30	1.27 ns
LVA to A_{area}	10	271%			–0.38 ns
$f_{mesophyll}$ to A_{area}	10	100%			0.11 ns
†A_{Chl} to A_{area}	9	561%	–1065%	–0.45, –0.72, 0.18	1.00 ns
Chl_{mes} to A_{area}	9	401%			0.39 ns
MVA to A_{area}	9	203%			–0.19 ns

n, species number; ***P<0.001; **P<0.01; *P<0.05; ns, not significant; asterisks indicate the significance of the slope parameter, i.e. whether the explanatory variable contributes significantly to the response variable (†: calculated parameter).
A_{area}, net CO_2 assimilation rate per unit leaf area; A_{Chl}, net CO_2 assimilation rate per chlorophyll; A_{mes}, net CO_2 assimilation rate per unit mesophyll; Chl_{mes}, chlorophyll concentration per mesophyll volume; D_{leaf}, leaf density; D_{leaf}*, leaf density corrected for porosity; f_{air}, intercellular airspace fraction; $f_{mesophyll}$, mesophyll fraction; *LMA*, leaf dry mass per area; $T_{epidermis,B}$, thickness of abaxial epidermis and hypodermis combined; $T_{epidermis,T}$, thickness of adaxial epidermis and hypodermis combined; T_{leaf}, leaf lamina thickness; $T_{mesophyll}$, mesophyll thickness.

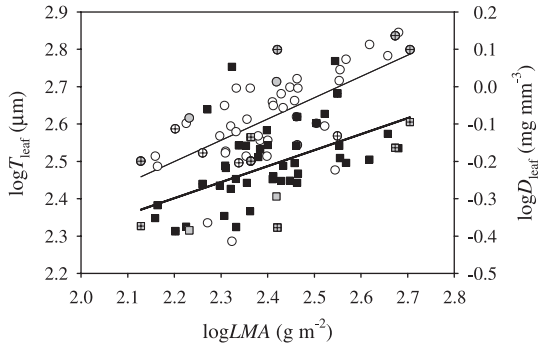

Fig. 2. Relationship between $\log_{10}$-transformed leaf lamina thickness (T_{leaf}, circles) or leaf density (D_{leaf}, squares) and leaf dry mass per area (*LMA*) in 49 *Banksia* species. Grey symbols show the seven species used for the measurement of mesophyll conductance, while crossed symbols represent the 10 species examined by microscopy (see Appendix for species names). [For the relationship between T_{leaf} and *LMA*, the slope is 0.57 and r^2 is 0.43 (P <0.001); for the relationship between D_{leaf} and *LMA*, the slope is 0.43 and r^2 is 0.30 (P <0.001).]

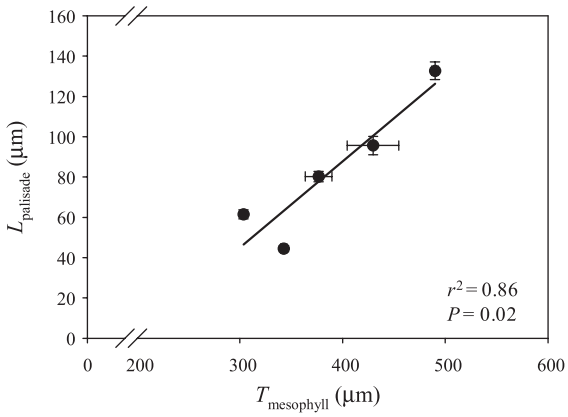

Fig. 3. Palisade cell length ($L_{palisade}$) against mesophyll thickness ($T_{mesophyll}$) in five *Banksia* species (see Appendix for species names).

Mesophyll tissue represented on average 74% of leaf lamina thickness (based on $T_{mesophyll}/T_{leaf}$) and 58% of leaf volume (based on *MVA*/*LVA*). High T_{leaf}, *LVA*, $T_{mesophyll}$, and *MVA* were associated with high *LMA* ($P \leq 0.01$) (data not shown). $T_{epidermis,T}$ varied 3-fold among the examined species and was significantly higher than $T_{epidermis,B}$ (P <0.001), which varied 2-fold. Both $T_{epidermis,T}$ and $T_{epidermis,B}$ increased with increasing *LMA*, although this was significant (P=0.008) only for $T_{epidermis,B}$ (data not shown).

Leaf density corrected for porosity (D_{leaf}*) tended to increase with increasing thickness of the different leaf layers, but none of these relationships were significant. The fraction of leaf occupied by air (f_{air}) tended to decrease with increasing thickness of the different leaf layers, although only its relationship with T_{leaf} was significant (P=0.016). f_{air} varied 3.5-fold among the species, ranging from 0.06 (in *B. elderiana*; T_{leaf}= 0.63 μm) to 0.22 (in *B. littoralis*; T_{leaf}=0.22 μm) (Fig. 4B). f_{air} was the only fraction of those examined that showed a significant (and negative) correlation with *LMA* (Fig. 4B). The mesophyll fraction ($f_{mesophyll}$) was ~0.6, irrespective of *LMA*, as was also the crypt fraction (f_{crypt}) of 0.1–0.2 (Fig. 4A). The epidermal fraction ($f_{epidermal}$) was 0.2–0.3 in all species examined (Fig. 4A) except for *B. repens* with a fraction of 0.1 and *B. ilicifolia* with a fraction of 0.4, which was indicative of the unusually thick adaxial epidermis and hypodermis of this species. Finally, the vascular tissue fraction ($f_{vascular}$) was 0.1–0.2, similar to f_{crypt}, for most species (Fig. 4A), although *B. repens* and *B. attenuata* showed a higher fraction of 0.3.

D_{leaf} was positively correlated with leaf dry matter content (r^2=0.28, P=0.023), which was similar but not quite significant for D_{leaf}*. D_{leaf}* contributed most to the variability of D_{leaf} (Table 1).

High-*LMA* leaves had significantly thicker mesophyll cell walls (T_w) (Fig. 5A). Thicker cell walls should impede CO_2 diffusion and were associated with lower mesophyll conductance (g_m) (Fig. 5B). Doubling T_w was associated with a halving in g_m.

Leaf structure, photosynthesis, and mesophyll conductance

The CO_2 assimilation rate per unit leaf area (A_{area}) and leaf conductance (g_{leaf}, which in the case of species with crypts

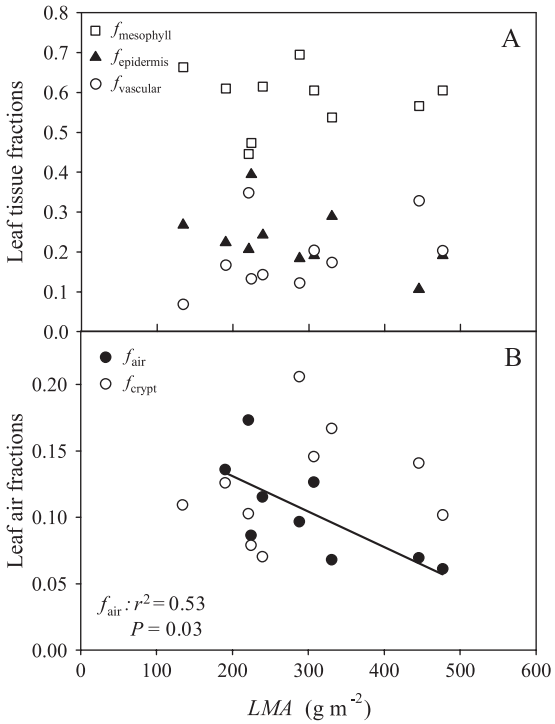

Fig. 4. Leaf fractions against leaf dry mass per area (*LMA*) in 10 *Banksia* species. (A) $f_{mesophyll}$, mesophyll fraction; $f_{epidermis}$, epidermal and hypodermal fraction; $f_{vascular}$, vascular tissue fraction. (B) f_{crypt}, crypt fraction; f_{air}, airspace fraction. Only f_{air} significantly and inversely correlated with *LMA*.

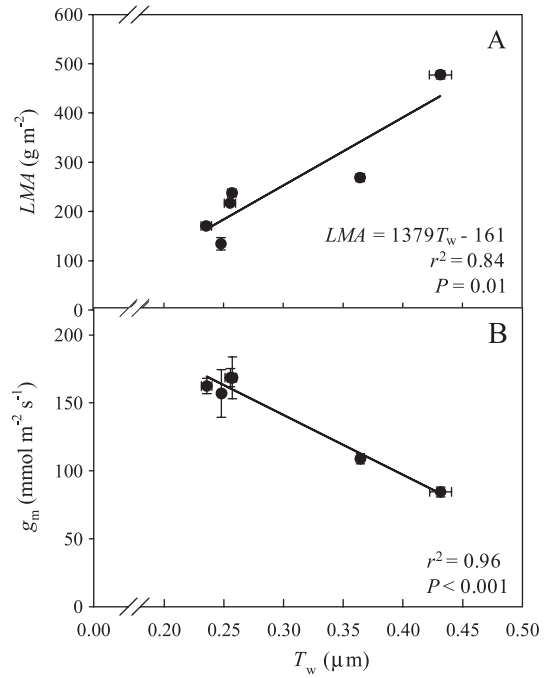

Fig. 5. Relationship of leaf dry mass per area (*LMA*) (A) and mesophyll conductance (g_m) (B) to mesophyll cell wall thickness (T_w) in six *Banksia* species (see Appendix for species names).

comprises stomatal and crypt conductance) correlated poorly with *LMA* (Fig. 6A, B), leaf thickness, and density (data not shown) in 18 species. In the subset of seven species in which mesophyll conductance (g_m) was measured, A_{area} and g_{leaf} tended to decrease with increasing *LMA*, while g_m strongly decreased with *LMA* (Fig. 6C). The decrease in g_m with increasing *LMA* that was observed in seven *Banksia* species was better correlated with D_{leaf} (r^2=0.76, P=0.01) than with T_{leaf} (r^2= 0.34, P=0.17). CO_2 assimilation rate per unit leaf mass (A_{mass}) showed a strong negative correlation with *LMA* (Fig. 7A), but not with T_{leaf} or D_{leaf} (data not shown). Nitrogen concentration (N_{mass}) varied 4-fold and decreased with increasing *LMA* (Fig. 7B). N_{mass} was rather low in all species (0.27–1.1%). As expected, A_{mass} was positively associated with N_{mass} (r^2=0.49, P=0.0018). No correlation was found between CO_2 assimilation rate per unit chlorophyll (A_{Chl}) and *LMA* (data not shown), while CO_2 assimilation rate per unit mesophyll (A_{mes}) decreased with increasing *LMA* (Fig. 8A). Factorizing A_{area} into CO_2 assimilation rate per unit mesophyll (A_{mes}), *LVA*, and $f_{mesophyll}$ showed that A_{mes} was more variable than the other parameters (Table 1). However, the large contribution of covariance, the negative correlations between A_{mes}, *LVA*, and $f_{mesophyll}$, and the non-significance of the slope analysis all indicate that further conclusions should not be drawn from these analyses. Factorizing A_{area} into the product of CO_2 assimilation rate per chlorophyll (A_{Chl}), chlorophyll concentration per mesophyll volume (Chl_{mes}), and mesophyll volume per unit leaf area (*MVA*), showed that A_{Chl} and Chl_{mes} were more variable than *MVA*, but the results also indicate that further conclusions should not be drawn from these analyses (Table 1).

CO_2 assimilation rate per unit nitrogen (*PNUE*) tended to decrease with increasing *LMA* (Fig. 8B). The fractions of nitrogen allocated to Rubisco and thylakoids tended to decrease with increasing *LMA*, although this was not significant (Fig. 9). Chlorophyll content per unit leaf area tended to be higher in high-*LMA* species with thicker mesophyll (r^2=0.22, P=0.08).

Discussion

Many comparative studies examining the variability in leaf structure and its effect on leaf physiology consider diverse species from different genera differing in *LMA* (Poorter and Evans, 1998; Wright *et al.*, 2004; Flexas *et al.*, 2008; Harrison *et al.*, 2009; Poorter *et al.*, 2009). In the present study, phylogenetic variation was minimized by focusing on one genus (*Banksia*) with a great leaf structural diversity that allowed quantitative relationships between *LMA* and its components to be established with photosynthetic characteristics at the high end of the *LMA* spectrum.

LMA and its anatomical correlates

Among the 49 *Banksia* species examined, *LMA* (134–507 g m^{-2}), T_{leaf} (193–700 μm), and D_{leaf} (0.41–1.17 mg mm^{-3})

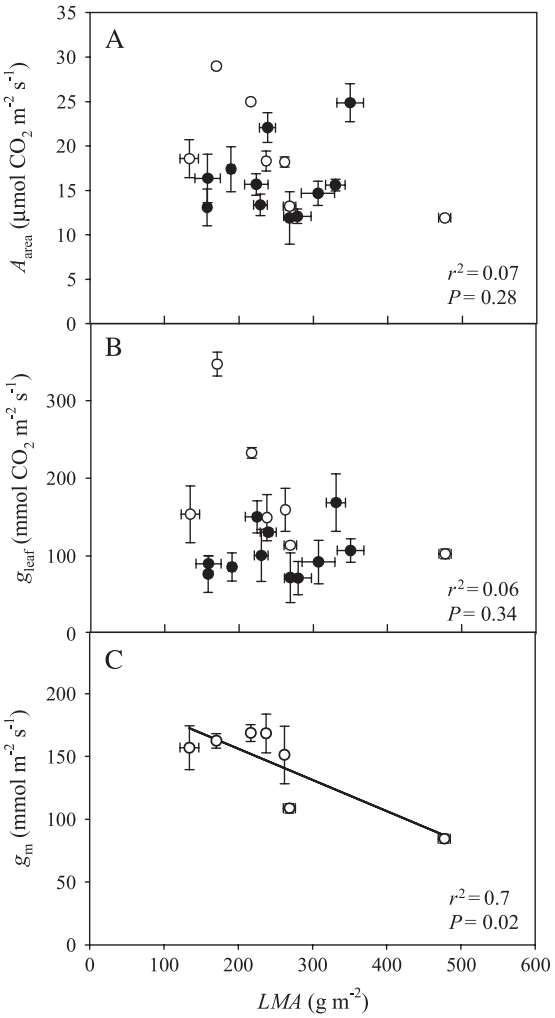

Fig. 6. Relationships of net CO_2 assimilation rate per unit leaf area (A_{area}) (A), leaf conductance (g_{leaf}: comprising stomatal conductance and crypt conductance in species with stomatal crypts) (B), and mesophyll conductance (g_m) (C) to leaf dry mass per area (*LMA*) in 18 *Banksia* species. Open circles, seven species in which g_m was measured; filled circles, all other species (see Appendix for species names). (C) Redrawn with permission from Hassiotou *et al.* (2009*a*).

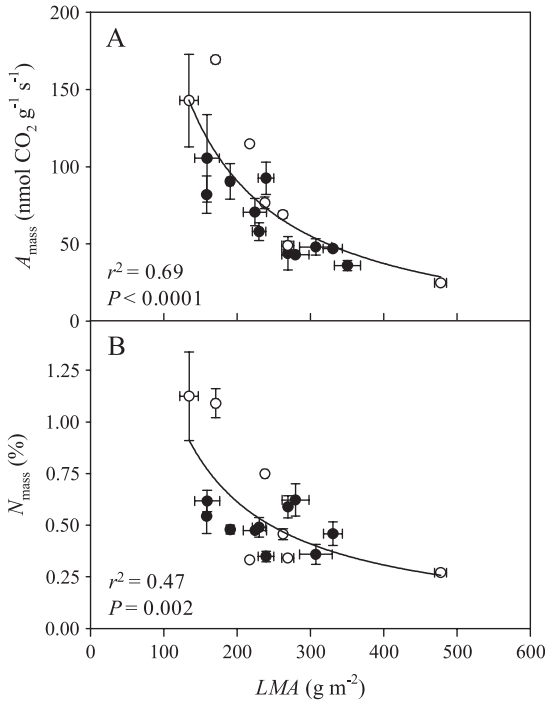

Fig. 7. Relationships of net CO_2 assimilation rate per unit leaf mass (A_{mass}) (A) and nitrogen content (N_{mass}) (B) to leaf dry mass per area (*LMA*) in 18 *Banksia* species. Open circles, seven species in which g_m was measured; filled circles, all other species (see Appendix for species names).

varied 4-, 4-, and 3-fold, respectively, which is indicative of the broad range of leaf structure that is represented in this genus. Niinemets *et al.* (2009) found a 4.7-fold variation in *LMA* (66–313 g m^{-2}) and a 2.5-fold variation in T_{leaf} (274–594 μm) and D_{leaf} (0.29–0.56 mg mm^{-3}) across 35 Australian sclerophyllous species from 20 genera. Poorter *et al.* (2009) reported a 4-fold variation in leaf volume per area (equivalent to T_{leaf}) (100–700 μm) and a 7-fold variation in D_{leaf} (0.1–0.6 mg mm^{-3}) in a data set containing woody and herbaceous species from three functional groups. In their data set, most of the variation in *LMA* within functional groups is attributed to variation in D_{leaf}, while differences in *LMA* between sclerophylls and mesophytes are usually due to variation in T_{leaf} (Poorter *et al.*, 2009). Log–log scaling slope analysis in species from three functional groups showed that 80% and 20% of the variability in *LMA* was due to variability in D_{leaf} and T_{leaf}, respectively (Poorter *et al.*, 2009). The larger role of D_{leaf} in the data set of Poorter *et al.* (2009) is due to the fact that the range in D_{leaf} was much greater in their data set than that in the 49 *Banksia* species examined in this study (7-fold and 3-fold, respectively), whereas the ranges in T_{leaf} were very similar (~4-fold in both data sets). Moreover, the relationship between D_{leaf} and *LMA* is fairly similar for different functional groups, whereas the relationship between T_{leaf} and *LMA* differs between functional groups, such that T_{leaf} becomes a poorer predictor of *LMA* in the combined data set. It is also noteworthy that values of D_{leaf}, T_{leaf}, and *LMA* of some of the *Banksia* species extend far beyond the range found in the data set of Poorter *et al.* (2009).

The considerable variability in both D_{leaf} and T_{leaf} in the present data set indicates that even within the same genus there are various ways of achieving high *LMA*, with potential ecological significance. Niinemets *et al.* (2009) found that density tended to increase with decreasing water availability, and thickness increased with decreasing soil fertility in a comparison of Australian species from sites that differed in water and nutrient availability. A number of previous studies have also reported increases in leaf thickness with decreasing soil fertility as well as with other factors, such as decreasing rainfall and humidity and increasing irradiance (Beadle, 1966; Nobel *et al.*, 1975; Chabot and Chabot, 1977; Givnish, 1978; Sobrado and Medina, 1980). High irradiance can result in increased T_{leaf} through the development of thicker epidermal tissues that confer photoprotection (Witkowski and Lamont, 1991;

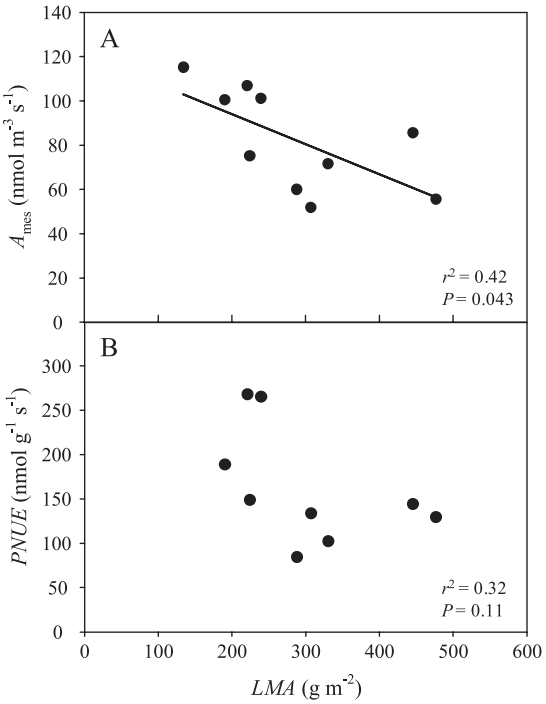

Fig. 8. Net CO_2 assimilation rate per unit mesophyll volume (A_{mes}) (n=10) (A) and photosynthetic nitrogen use efficiency (*PNUE*) (n=9) (B) against leaf dry mass per area (*LMA*) in 9–10 *Banksia* species (see Appendix for species names).

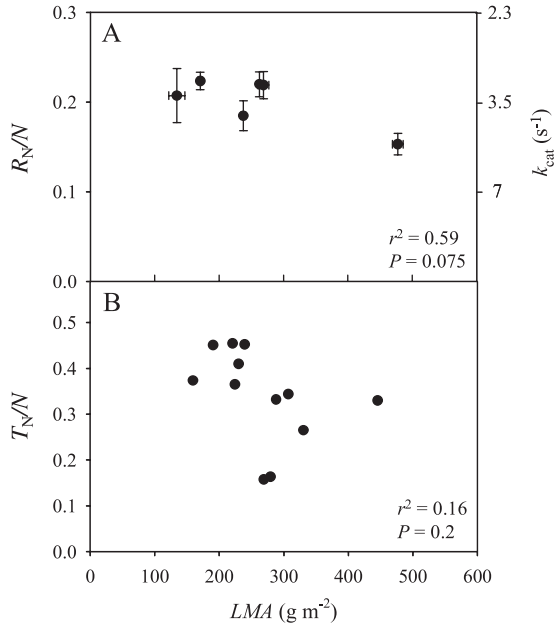

Fig. 9. Fraction of nitrogen allocated to Rubisco (R_N/N) (A) and to thylakoids (T_N/N) (B) against leaf dry mass per area (*LMA*) in six and 12 *Banksia* species, respectively (see Appendix for species names). For R_N/N, a k_{cat} value of 3.5 mol CO_2 (mol Rubisco sites)$^{-1}$ s^{-1} was used. The right *y*-axis in (A) shows the predicted k_{cat} value assuming a constant R_N/N of 0.2.

Jordan *et al.*, 2005). High irradiance can also lead to high D_{leaf} (Chabot and Chabot, 1977) through addition of dense, sclerified tissues that increase the uniformity of illumination within thick leaves (Poulson and Vogelmann, 1990; Karabourniotis, 1998), although these tissues may also play other roles, such as providing support and enhancing the rigidity of long-lived high-*LMA* leaves.

D_{leaf}* was an important predictor of *LMA* in *Banksia* leaves. Increases in D_{leaf}* can result from increases in the proportion of non-photosynthetic supporting tissue, especially sclerified cells, and/or a general tendency for cells to have more structural mass. The latter can be due to thicker cell walls, but also to larger surface to volume ratios of smaller cells. In *Banksia*, mesophyll cells of high-*LMA* species had thicker cell walls compared with low-*LMA* species: a 4-fold range in *LMA* was accompanied by a 2-fold range in T_w. This demonstrates that *LMA* does not simply scale proportionally with T_w. Previous studies have reported a range of 0.15–0.4 μm for T_w (Hanba *et al.*, 1999, 2001, 2002), with the *Banksia* species examined here being at the high end of this range, but with much higher *LMA* than the tree leaf *LMA* values from the above studies. Interestingly, the fraction of leaf volume occupied by the mesophyll was independent of *LMA*, indicating that high-*LMA* leaves used greater mesophyll volumes to achieve similar photosynthetic rates per unit leaf area to those of low-*LMA* leaves. As with the mesophyll fraction, the crypt, epidermal, and vascular tissue fractions were all independent of *LMA*, demonstrating that the volume of these tissues scales with leaf volume across a wide range of *LMA*. The decrease in mesophyll airspace fraction at high *LMA* was associated with the presence of larger and deeper stomatal crypts, which may facilitate diffusion by locally reducing the distance between the stomata and the adaxial palisade cells (Hassiotou *et al.*, 2009*b*).

Leaf thickening can occur through (i) addition of mesophyll cell layers; (ii) elongation of mesophyll cells; and/or (iii) addition of non-photosynthetic supporting tissue in the epidermal and hypodermal layers. The present results indicate that, in *Banksia*, all tissues contribute somewhat to increases in T_{leaf}, but $T_{mesophyll}$ contributes the most and is a better predictor of T_{leaf} than the epidermal thicknesses. Microscopic observations suggest that elongation of adaxial palisade cells was a major contributor to mesophyll thickening (Fig. 3). Abaxial palisade-like cells were observed in *Banksia* leaves alongside the crypts, a pattern that appears to be more common in high-*LMA* leaves, but more research is needed to elucidate their contribution to leaf thickening.

Given that A_{area} and $f_{mesophyll}$ did not correlate with *LMA*, a question arises as to whether this indicates that the increase in mesophyll volume per area with increasing *LMA* is associated with a roughly proportional decrease in photosynthesis per unit mesophyll. Are there limits to how much photosynthetic tissue per area a leaf can have before it becomes inefficient in some way?

Leaf structure, photosynthesis, and mesophyll conductance

LMA has often been the trait of interest when looking at relationships between leaf structure and photosynthesis, but

since it is a product of two anatomical traits that often vary independently (T_{leaf} and D_{leaf}) and that may influence photosynthesis differently, a great variability is found in the relationship between *LMA* and A_{area} (Niinemets and Sack, 2006), which was also observed among *Banksia* species in this study. In contrast, a clearer negative relationship exists between A_{mass} and *LMA* (Fig. 7A; Wright *et al.*, 2004). This can be at least partly attributed to the fact that high-*LMA* species have more structural material per unit dry mass, as indicated through their higher dry matter content.

Few studies have examined how the two components of *LMA*, D_{leaf} and T_{leaf}, relate to photosynthetic rates. In the present study, neither D_{leaf} nor T_{leaf} strongly correlated with A_{area} or A_{mass}. In a meta-analysis in a large data set, Niinemets (1999) found no significant relationship between A_{area} and D_{leaf}, but A_{area} scaled with T_{leaf} and *LMA*, while A_{mass} scaled negatively with D_{leaf} and *LMA*, being independent of T_{leaf}. While D_{leaf} and T_{leaf} are appealing parameters because they are easy to measure, their poor explanatory power suggests that other leaf traits that are more difficult to obtain are required to explain variation in photosynthetic rates.

The lower A_{mass} in combination with the lower N_{mass} at high *LMA* can explain the weak relationship obtained between *PNUE* (*PNUE*=A_{mass}/N_{mass}) and *LMA*. This is in contrast to previous studies, which reported a strong decrease of *PNUE* with increasing *LMA* (Poorter and Evans, 1998; Hikosaka, 2004), attributing this relationship to the lower N_{area} and higher Rubisco specific activity of low-*LMA* leaves, and the increased allocation of nitrogen to non-photosynthetic (structural) relative to photosynthetic (e.g. Rubisco) components in high-*LMA* leaves. However, Harrison *et al.* (2009), in a comprehensive study of 25 species covering a 10-fold range in *LMA*, showed that the fraction of nitrogen allocated to cell walls is independent of *LMA*. Moreover, they found that the relationship between the fraction of nitrogen allocated to Rubisco and *LMA* is curvilinear: at low *LMA*, the fraction of nitrogen associated with Rubisco decreases with *LMA*—explaining the negative correlation between *PNUE* and *LMA* that has been found in previous studies—down to a stable level above an *LMA* of 130 g m^{-2}. All the *Banksia* species examined in the present study had *LMA* >134 g m^{-2}; thus, the absence of a strong correlation between *PNUE* and *LMA* in these species is consistent with the findings of Harrison *et al.* (2009). Interestingly, *PNUE* was high compared with previous studies on other species (Reich *et al.*, 1991; Sobrado, 2009). This is similar to the finding of high photosynthetic phosphorus use efficiency in *Banksia* species (Denton *et al.*, 2007). The physiological basis for these high nutrient use efficiencies is unresolved, but the adaptation is presumably vital for these species, which occur on some of the most nutrient-impoverished soils in the world (Richardson *et al.*, 2004).

The observed low N_{mass} is consistent with the species' high *LMA* and their oligotrophic habitats (Reich *et al.*, 1991; Wright and Cannon, 2001; Niinemets *et al.*, 2009). High-*LMA* species had higher N_{area} and lower N_{mass}, with the latter being more strongly correlated with *LMA*. This is in agreement with the global trends (Wright *et al.*, 2004). Since a large percentage of leaf N is directly associated with the photosynthetic machinery (Wright *et al.*, 2004), the negative relationship between N_{mass} and *LMA* is probably due to the more numerous thick-walled cells and sclerified tissues in high-*LMA* leaves, and is consistent with the general trend of species at the high-*LMA* end of the spectrum (Wright *et al.*, 2004). It would be worthwhile to measure *N* concentrations of mesophyll tissue across the range of *LMA*. The present data do not enable an estimation to be made of the mesophyll *N* concentrations; however, *Chl* per mesophyll volume was estimated based on the assumption that all leaf chlorophyll is located in the mesophyll. Chl_{mes} did not significantly decrease with increasing *LMA*. A similar pattern or a slight decrease with *LMA* (given the reduction in A_{mes} with *LMA*) may be expected for *N* per mesophyll volume.

An increasing body of evidence shows that g_m is an important factor limiting photosynthesis in C_3 plants (Flexas *et al.*, 2008; Evans *et al.*, 2009). In seven *Banksia* species, g_m decreased significantly with increasing *LMA* (Fig. 6C and Hassiotou *et al.*, 2009*a*). The negative relationship between g_m and *LMA* was mainly associated with D_{leaf} and not with T_{leaf}, since the latter correlated poorly with g_m. A factor contributing to the increase in D_{leaf} and directly to g_m was the increase in mesophyll cell wall thickness (Fig. 5B).

A_{mes}, A_{Chl}, and Chl_{mes} were better predictors and contributed more to the variability of A_{area} than $f_{mesophyll}$ and *MVA* (although none of the corresponding slope analyses were significant) and these trends indicate that the photosynthetic capacity of the tissue is more responsible for the variation in A_{area} than the amounts of photosynthetically active tissue. Interestingly, A_{area} in the examined species reached values that were comparable with many mesophytic species of lower *LMA* (Flexas *et al.*, 2008). Denton *et al.* (2007) found similar photosynthetic rates in field-grown *Banksia* plants.

A_{mes} decreased as *LMA* increased, since *MVA* increased with *LMA*. The chloroplastic CO_2 concentration (C_c) was remarkably stable across the *LMA* range examined (Hassiotou *et al.*, 2009*a*), so this does not explain a lower A_{mes}. Evans *et al.* (2009) reported a positive relationship between mesophyll resistance per unit of exposed chloroplast surface area and mesophyll cell wall thickness (T_w), and a negative relationship between the rates of photosynthesis per unit of exposed chloroplast surface area, A_c, and T_w. To the extent that A_{mes} reflects A_c, the data for *Banksia* confirm this trend. Lower A_{mes} may offset the impact of the increase in T_w in high-*LMA* leaves to moderate the CO_2 drawdown from the substomatal cavity to the sites of carboxylation. A similar relationship was found by Terashima *et al.* (2006). Evidence suggests that at the high-*LMA* end of the spectrum, investment in chlorophyll is not a key component of A_{mes}. Instead, the lower A_{mes} of high-*LMA* leaves may reflect lower Rubisco

concentrations, lower Rubisco specific activity, lower Rubisco activation state, or reduced nitrogen allocation. The decreasing trend between *PNUE* (Fig. 8B) or nitrogen allocation to Rubisco or thylakoids (Fig. 9) and *LMA* suggests that reduced allocation of nitrogen to photosynthetic proteins may be causing the decline in A_{mes}. In *Banksia*, greater investment in photosynthetic machinery may not be advantageous in the extremely nutrient-impoverished and seasonally dry habitats of these species where economic use of nutrients is vital and partial stomatal closure is common in the dry season (Veneklaas and Poot, 2003).

In addition to lower investment in photosynthetic machinery, lower A_{mes} in high-*LMA* leaves could be a consequence of structural changes that result in irregular distribution of CO_2 and light across the leaf or greater diffusive limitations. For example, mesophyll cell wall thickness, which was greater in high-*LMA* leaves, may compromise g_m. Mesophyll surface area exposed to the intercellular spaces is another component of g_m which needs to be measured in order to understand the anatomical basis of g_m. Difficulty in embedding the *Banksia* leaves has so far prevented this important parameter from being obtained. A meta-analysis showed that leaf structure was a more important determinant of photosynthesis than nitrogen (Niinemets, 1999).

There are some anatomical and physiological mechanisms that may reduce the negative effects of the structure of thick and dense leaves on CO_2 diffusion and light transmission. Increased presence of bundle sheath extensions and other sclerenchymatous tissues in high-*LMA* leaves facilitates light transmission to deeper leaf layers (Poulson and Vogelmann, 1990; Smith *et al.*, 1997; Karabourniotis, 1998; Nikolopoulos *et al.*, 2002), improving the uniformity of illumination across thick leaves. Stomatal crypts, present in most *Banksia* species (Hassiotou *et al.*, 2009*b*), facilitate CO_2 diffusion to adaxial palisade cells.

Conclusions

The detailed analyses of the specific leaf structural and physiological traits contributing to variation in A_{area} in *Banksia* leaves have provided new insights into the relationship between A_{area} and *LMA* at the high end of the *LMA* spectrum. These leaves have large amounts of dense tissues that are not photosynthetically active, and therefore it is not surprising that they have lower A_{mass}. The present analysis of the factors that contribute to variation in A_{area}, however, shows that high-*LMA* leaves actually have more mesophyll per unit leaf area, but that the photosynthetic capacity of this tissue is lower. The net result is that photosynthetic rates per unit leaf area are independent of *LMA*. The lower photosynthetic capacity of the mesophyll of high-*LMA* leaves in *Banksia* could be due to structural limitations and partly to lower nitrogen concentrations. The contribution from these two limitations to the reduction of A_{mes} at high *LMA* may differ between species. Future research must focus on how structural components (e.g. mesophyll surface area exposed to the intercellular airspaces) and the investment in photosynthetic machinery (e.g. Rubisco and nitrogen allocation to mesophyll) change with *LMA*, as potential explanations of the lower A_{mes} of high-*LMA* leaves.

Acknowledgements

The authors would like to acknowledge the Centre for Microscopy, Characterisation and Analysis (CMCA) of the University of Western Australia, where most microscopic analyses were carried out. Many thanks are extended to Dr Cheng Huang, who assisted with the cryo-scanning electron microscopy carried out at the Electron Microscopy Unit (EMU) of the Australian National University. This part of the study was funded by a Grieve Memorial Travel grant and a Robertson Fellowship for FH. The authors are grateful to Professor Hans Lambers, Dr Hendrik Poorter, and two anonymous reviewers for their comments on an earlier version of this manuscript. During this study FH was the recipient of an Australian Postgraduate Award.

Appendix

List of the 49 *Banksia* species examined (for nomenclature see Western Australian Herbarium, 1998)

	Analysis									
Species	**1**	**2**	**3**	**4**	**5**	**6**	**7**	**8**	**9**	**10**
B. aculeata	+									
B. aemula	+									
B. ashbyi	+									
B. attenuata	+	+	+	+	+	+	+	+	+	
B. baueri	+									
B. baxteri	+									
B. benthamiana	+									
B. brownii	+									
B. burdettii	+									
B. caleyi	+									
B. candolleana	+	+	+	+	+	+				
B. chamaephyton	+									
B. coccinea	+	+	+	+	+					
B. dentata	+									
B. dryandroides	+	+								
B. elderiana	+	+	+	+		+	+	+	+	+
B. elegans	+									
B. epica	+									
B. gardneri	+									
B. goodii	+									
B. grandis	+									
B. hookeriana	+	+	+	+	+	+			+	
B. ilicifolia	+	+	+	+	+	+			+	
B. integrifolia	+	+	+				+	+		+
B. laevigata	+									
B. lemanniana	+									
B. lindleyana	+									

Table . *Continued*

Species	Analysis 1	2	3	4	5	6	7	8	9	10
B. littoralis	+	+	+	+	+					
B. media	+									
B. menziesii	+									
B. oblongifolia	+									
B. oligantha	+									
B. oreophila	+	+	+	+	+					
B. paludosa	+	+	+				+			+
B. petiolaris	+									
B. pilostylis	+									
B. praemorsa	+									
B. prionotes	+	+	+	+	+	+				
B. quercifolia	+	+	+	+						
B. repens	+	+	+	+	+	+	+	+		+
B. rosserae	+									
B. sceptrum	+									
B. seminuda	+									
B. serrata	+	+	+			+	+	+		+
B. solandri	+	+	+	+	+	+	+	+	+	+
B. speciosa	+									
B. spinulosa	+	+	+	+	+					
B. verticillata	+									
B. victoriae	+	+	+	+	+	+				

1: 49 species (Fig. 1), leaf dry mass per area and its relationship with leaf density and thickness, 2: 18 species (Figs 5a, b, 6a), gas exchange measurements (CO_2 assimilation rate and leaf conductance); 3: 17 species (Fig. 6b, c), nitrogen content and photosynthetic nitrogen use efficiency; 4: 14 species (Fig. 3a), leaf volume and porosity; 5: 12 species (Fig. 8b), nitrogen allocated to thylakoids; 6: 10 species (Figs 2a, 3b, 7), thickness of the different leaf layers, mesophyll volume per unit leaf volume, and net CO_2 assimilation rate per unit mesophyll; 7: 7 species (Fig. 5c), mesophyll conductance; 8: 6 species (Fig. 4), mesophyll cell wall thickness; 9: 5 species (Fig. 2b), palisade cell length; 10: 6 species (Fig. 8a), nitrogen allocated to Rubisco.

References

Abramoff MD, Magelhaes PJ, Ram SJ. 2004. Image processing with Image J. *Biophotonics International* **11,** 36–42.

Baldini E, Facini O, Nerozzi F, Rossi F, Rotondi A. 1997. Leaf characteristics and optical properties of different woody species. *Trees* **12,** 73–81.

Beadle NCW. 1966. Soil phosphate and its role in molding segments of the Australian flora and vegetation, with special reference to xeromorphy and sclerophylly. *Ecology* **47,** 992–1007.

Chabot BF, Chabot JF. 1977. Effects of light and temperature on leaf anatomy and photosynthesis in *Fragaria vesca*. *Oecologia* **26,** 363–377.

Chapin FS. 1980. The mineral nutrition of wild plants. *Annual Review of Ecology and Systematics* **11,** 233–260.

Denton MD, Veneklaas EJ, Freimoser FM, Lambers H. 2007. *Banksia* species (Proteaceae) from severely phosphorus-impoverished soils exhibit extreme efficiency in the use and re-mobilisation of phosphorus. *Plant, Cell and Environment* **30,** 1557–1565.

Dillon RJ. 2002. The diversity of scleromorphic structures in the leaves of Proteaceae. Honours thesis. Hobart, Australia: University of Tasmania.

Evans JR. 1989. Photosynthesis and nitrogen relationships in leaves of C_3 plants. *Oecologia* **78,** 9–19.

Evans JR, Kaldenhoff R, Genty B, Terashima I. 2009. Resistances along the CO_2 diffusion pathway inside leaves. *Journal of Experimental Botany* **60,** 2235–2248.

Evans JR, Loreto F. 2000. Acquisition and diffusion of CO_2 in higher plant leaves. In: Leegood RC, Sharkey TD, von Caemmerer S, eds. *Photosynthesis: physiology and metabolism*. Dordrecht, The Netherlands: Kluwer Academic Publishers, 321–351.

Evans JR, von Caemmerer S. 1996. Carbon dioxide diffusion inside leaves. *Plant Physiology* **110,** 339–346.

Evans JR, von Caemmerer S, Setchell BA, Hudson GS. 1994. The relationship between CO_2 transfer conductance and leaf anatomy in transgenic tobacco with reduced content of Rubisco. *Australian Journal of Plant Physiology* **21,** 475–495.

Flexas J, Ribas-Carbo M, Diaz-Espejo A, Galmés J, Medrano H. 2008. Mesophyll conductance to CO_2: current knowledge and future prospects. *Plant, Cell and Environment* **31,** 601–621.

Givnish TJ. 1978. Ecological aspects of plant morphology: leaf form in relation to environment. In: Satteer R, ed. *Theoretical plant morphology* (*Acta Biotheoretica,* Vol. 27*)*. The Hague, The Netherlands: Linden University Press, 83–142.

Hanba YT, Kogami H, Terashima I. 2002. The effect of growth irradiance on leaf anatomy and photosynthesis in *Acer* species differing in light demand. *Plant, Cell and Environment* **25,** 1021–1030.

Hanba YT, Miyazawa S-I, Kogami H, Terashima I. 2001. Effects of leaf age on internal CO_2 transfer conductance and photosynthesis in tree species having different types of shoot phenology. *Australian Journal of Plant Physiology* **28,** 1075–1084.

Hanba YT, Miyazawa S-I, Terashima I. 1999. The influence of leaf thickness on the CO_2 transfer conductance and leaf stable carbon isotope ratio for some evergreen tree species in Japanese warm temperate forests. *Functional Ecology* **13,** 632–639.

Harley PC, Loreto F, Di Marco G, Sharkey TD. 1992. Theoretical considerations when estimating the mesophyll conductance to CO_2 flux by the analysis of the response of photosynthesis to CO_2. *Plant Physiology* **98,** 1429–1436.

Harrison MT, Edwards EJ, Farquhar GD, Nicotra AB, Evans JR. 2009. Nitrogen in cell walls of sclerophyllous leaves accounts for little of the variation in photosynthetic nitrogen-use efficiency. *Plant, Cell and Environment* **32,** 259–270.

Hassiotou F, Evans JR, Martha L, Veneklaas EJ. 2009*b*. Stomatal crypts may facilitate diffusion of CO_2 to adaxial mesophyll cells in thick sclerophylls. *Plant, Cell and Environment* **32,** 1596–1611.

Hassiotou F, Ludwig M, Renton M, Veneklaas EJ, Evans JR. 2009*a*. Influence of leaf dry mass per area, CO_2 and irradiance on mesophyll conductance in sclerophylls. *Journal of Experimental Botany* **60,** 2303–2314.

Hikosaka K. 2004. Interspecific difference in the photosynthesis–nitrogen relationship: patterns, physiological causes, and ecological importance [review]. *Journal of Plant Research* **117,** 481–494.

Jordan GJ, Dillon RA, Weston PH. 2005. Solar radiation as a factor in the evolution of scleromorphic leaf anatomy in Proteaceae. *American Journal of Botany* **92,** 789–796.

Karabourniotis G. 1998. Light-guiding function of foliar sclereids in the evergreen sclerophyll *Phillyrea latifolia*: a quantitative approach. *Journal of Experimental Botany* **49,** 739–746.

Loreto F, Harley PC, Di Marco G, Sharkey TD. 1992. Estimation of mesophyll conductance to CO_2 flux by three different methods. *Plant Physiology* **98,** 1437–1443.

Mast AR, Givnish TJ. 2002. Historical biogeography and the origin of stomatal distributions in *Banksia* and *Dryandra* (Proteaceae) based on their cpDNA phylogeny. *American Journal of Botany* **89,** 1311–1323.

McCully ME, Canny MJ, Huang CX. 2004. The management of extracellular ice by petioles of frost-resistant herbaceous plants. *Annals of Botany* **94,** 665–674.

Myers DA, Vogelmann TC, Bornman JF. 1994. Epidermal focusing and effects on light utilization in *Oxalis acetosella*. *Physiologia Plantarum* **91,** 651–656.

Niinemets Ü. 1999. Research review. Components of leaf dry mass per area—thickness and density—alter leaf photosynthetic capacity in inverse directions in woody plants. *New Phytologist* **144,** 35–47.

Niinemets Ü, Sack L. 2006. Structural determinants of leaf light-harvesting capacity and photosynthetic potentials. *Progress in Botany* **67,** 385–419.

Niinemets Ü, Wright IJ, Evans JR. 2009. Leaf mesophyll diffusion conductance in 35 Australian sclerophylls covering a broad range of foliage structural and physiological variation. *Journal of Experimental Botany* **60,** 2433–2449.

Nikolopoulos D, Liakopoulos G, Drossopoulos I, Karabourniotis G. 2002. The relationship between anatomy and photosynthetic performance of heterobaric leaves. *Plant Physiology* **129,** 235–243.

Nobel PS, Zaragoza LJ, Smith WK. 1975. Relation between mesophyll surface area, photosyuthetic rate, and illumination level during development for leaves of *Plectranthus parviflorus* Henckel. *Plant Physiology* **55,** 1067–1070.

Parkhurst DF. 1994. Diffusion of CO_2 and other gases inside leaves. *New Phytologist* **126,** 449–479.

Poorter H, Evans JR. 1998. Photosynthetic nitrogen-use efficiency of species that differ inherently in specific leaf area. *Oecologia* **116,** 26–37.

Poorter H, Niinemets Ü, Poorter L, Wright IJ, Villar R. 2009. Causes and consequences of variation in leaf mass per area (LMA): a meta-analysis. *New Phytologist* **182,** 565–588.

Poorter H, van der Werf A. 1998. Is inherent variation in RGR determined by LAR at low irradiance and by NAR at high irradiance? A review of herbaceous species. In: Lambers H, Poorter H, van Vuuren MMI, eds. *Inherent variation in plant growth*. Leiden, The Netherlands: Backhuys Publishers, 309–336.

Poulson ME, Vogelmann TC. 1990. Epidermal focusing and effects upon photosynthetic light-harvesting in leaves of *Oxalis*. *Plant, Cell and Environment* **13,** 803–811.

Raskin I. 1983. A method for measuring leaf volume, density, thickness and internal gas volume. *Hortscience* **18,** 698–699.

Read J, Edwards C, Sanson GD, Aranwela N. 2000. Relationships between sclerophylly, leaf biomechanical properties and leaf anatomy in some Australian heath and forest species. *Plant Biosystems* **134,** 261–277.

Read J, Sanson GD. 2003. Characterizing sclerophylly: the mechanical properties of a diverse range of leaf types. *New Phytologist* **160,** 81–99.

Reich PB, Uhl C, Walters MB, Ellsworth DS. 1991. Leaf lifespan as a determinant of leaf structure and function among 23 Amazonian tree species. *Oecologia* **86,** 16–24.

Reich PB, Walters MB, Ellsworth DS. 1997. From tropics to tundra: global convergence in plant functioning. *Proceedings of National Academy of Sciences, USA* **94,** 13730–13734.

Richardson SJ, Peltzer DA, Allen RB, McGlone MS, Parfitt RL. 2004. Rapid development of phosphorus limitation in temperate rainforest along the Franz Josef soil chronosequence. *Oecologia* **139,** 267–276.

Sharkey TD, Bernacchi CJ, Farquhar GD, Singsaas EL. 2007. Fitting photosynthetic carbon dioxide response curves for C3 leaves. *Plant, Cell and Environment* **30,** 1035–1040.

Smith WK, Vogelmann TC, DeLucia EH, Bell DT, Shepherd KA. 1997. Leaf form and photosynthesis. Do leaf structure and orientation interact to regulate internal light and carbon dioxide? *Bioscience* **47,** 785–793.

Sobrado MA. 2009. Cost-benefit relationships in sclerophyllous leaves of the 'Bana' vegetation in the Amazon region. *Trees* **23,** 429–437.

Sobrado MA, Medina E. 1980. General morphology, anatomical structure, and nutrient content of sclerophyllous leaves of 'the Bana' vegetation of Amazonas. *Oecologia* **45,** 341–345.

Terashima I, Hanba YT, Tazoe Y, Vyas P, Yano S. 2006. Irradiance and phenotype: comparative eco-development of sun and shade leaves in relation to photosynthetic CO_2 diffusion. *Journal of Experimental Botany* **57,** 343–354.

Thomson CJ, Armstrong W, Waters I, Greenway H. 1990. Aerenchyma formation and associated oxygen movement in seminal and nodal roots of wheat. *Plant, Cell and Environment* **13,** 395–403.

Turner IM. 1994. Sclerophylly: primarily protective? *Functional Ecology* **8,** 669–675.

Veneklaas EJ, Poot P. 2003. Seasonal patterns in water use and leaf turnover of different plant functional types in a species-rich woodland, south-western Australia. *Plant and Soil* **257,** 295–304.

von Caemmerer S, Evans JR, Hudson GS, Andrews TJ. 1994. The kinetics of ribulose 1,5-bisphosphate carboxylase/oxygenase *in vivo* inferred from measurements of photosynthesis in leaves of transgenic tobacco. *Planta* **195,** 88–97.

Wellburn AR. 1994. The spectral determination of chlorophylls a and b, as well as total carotenoids, using various solvents with spectrophotometers of different resolution. *Journal of Plant Physiology* **144,** 307–313.

Western Australian Herbarium. 1998. FloraBase – The Western Australian Flora. Department of Environment and Conservation. http://florabase.dec.wa.gov.au/

Westoby M, Falster DS, Moles AT, Vesk PA, Wright IJ. 2002. Plant ecological strategies: some leading dimensions of variation between species. *Annual Review of Ecology and Systematics* **33,** 125–159.

Witkowski ETF, Lamont BB. 1991. Leaf specific mass confounds leaf density and thickness. *Oecologia* **88,** 486–493.

Wright IJ, Cannon K. 2001. Relationships between leaf lifespan and structural defences in a low-nutrient, sclerophyll flora. *Functional Ecology* **15,** 351–359.

Wright IJ, Reich BP, Westoby M, *et al*. 2004. The worldwide leaf economics spectrum. *Nature* **428,** 821–827.